materials proceedings

MDPI

Proceeding Paper

Synthesis, Suspension Stability, and Bioactivity of Curcumin-Carrying Chitosan Polymeric Nanoparticles †

Manuel Iza-Anaya, César Uriel Rodríguez-Fuentes, Abigail Varela-Pérez and Cynthia Cano-Sarmiento *

Unidad de Investigación y Desarrollo en Alimentos, Tecnológico Nacional de México/Instituto Tecnológico de Veracruz, Veracruz 91897, Mexico; izaanayamanuel@gmail.com (M.I.-A.); cesarrodriguef@hotmail.com (C.U.R.-F.); abigail_2365@hotmail.com (A.V.-P.)

* Correspondence: cynthia.cs@veracruz.tecnm.mx

† Presented at the International Symposium on Nanotechnology for Medicine, Environment and Energy, Veracruz, Mexico, 5–7 November 2025.

Abstract

Curcumin is a phenolic compound with antioxidant and anti-inflammatory properties; however, due to its low bioavailability, the use of encapsulation systems is recommended. Chitosan-based polymeric nanoparticles produced via ionic gelation offer controlled release, though their storage stability remains limited. In this work, the incorporation of collagen-derived peptides, NaCl, and Tween® 80 was evaluated as a strategy to enhance physicochemical performance. A 2^3 factorial design was used to identify the most relevant formulation components, resulting in four stable systems capable of retaining curcumin and preserving its antioxidant and anti-inflammatory activity during storage. These findings highlight the potential of chitosan-based systems for improving the functional performance of curcumin and suspension stability.

Keywords: Curcumin; Chitosan nanoparticles; Encapsulation; Stability; Bioactivity

check for updates

Academic Editors: Luis Zamora-Peredo and Marcos Luna-Cervantes

Published: 17 December 2025

Citation: Iza-Anaya, M.; Rodríguez-Fuentes, C.U.; Varela-Pérez, A.; Cano-Sarmiento, C. Synthesis, Suspension Stability, and Bioactivity of Curcumin-Carrying Chitosan Polymeric Nanoparticles. *Mater. Proc.* **2025**, *28*, 6. https://doi.org/10.3390/materproc2025028006

Copyright: © 2025 by the authors. Licensee MDPI, Basel, Switzerland. This article is an open access article distributed under the terms and conditions of the Creative Commons Attribution (CC BY) license (https://creativecommons.org/licenses/by/4.0/).

1. Introduction

Curcumin, the primary phenolic compound in the rhizomes of *Curcuma longa* (turmeric), exhibits diverse pharmacological activities, including antiviral, anticancer, antioxidant, and anti-inflammatory effects [1,2]. At the cellular level, these effects are mediated by the modulation of signaling pathways, such as the inhibition of pro-inflammatory cytokines, free radical scavenging, and the induction of antioxidant enzymes [3,4]. Despite its therapeutic potential, curcumin's low bioavailability limits its clinical effectiveness, motivating the development of delivery systems that enhance stability, bioavailability, and bioactivity [5,6].

Polymeric nanoparticles are particularly promising for the application of curcumin encapsulation due to their small size (10–500 nm), colloidal nature, and capacity to form protective matrices [7–9]. Of the methods for polymeric nanoparticles, ionic gelation is preferred, as it relies on electrostatic interactions between polymers such as chitosan and crosslinkers such as sodium tripolyphosphate (TPP) to form pH-responsive nanoparticles [10,11]. Although chitosan–TPP systems offer the benefits of biocompatibility and low toxicity, and are widely used, challenges such as water-induced swelling, structural instability, and high polydispersity can compromise long-term storage stability and controlled release performance [12–14]. To address these limitations, stabilizing components such as collagen-derived peptides have been incorporated to reinforce the chitosan matrix through ionic and hydrogen bond interactions without affecting its pH-responsive behavior [15].

Similarly, salts and surfactants can modulate particle formation and reduce size variability, though their influence on structural integrity and curcumin bioactivity requires careful consideration [16,17].

Even with these advances, few studies assess how multiple formulation factors interact to determine stability, encapsulation, and biological performance. Therefore, this study evaluates the combined effects of collagen peptides, NaCl, and Tween® 80 using a 2^3 factorial design, providing a clearer understanding of the parameters that optimize chitosan-based carriers for curcumin delivery.

2. Materials and Methods

2.1. Materials

All solvents were of analytical or HPLC grade. Chitosan (high molecular weight, 96% deacetylation) was obtained from Encapsuladoras México (Chihuahua, Mexico); sodium tripolyphosphate (TPP) from NINU.MX (Xalapa, Mexico); type I and II collagen peptides from Natsa (Chihuahua, Mexico); curcumin from LKT Laboratories (St. Louis, MO, USA); and Tween 80® and NaCl from Sigma Aldrich (St. Louis, MO, USA).

2.2. Nanoparticle Synthesis

Nanoparticles were synthesized by ionic gelation. Chitosan solution was prepared by dissolving 0.2 g in 100 mL of 1% *v/v* acetic acid, followed by stirring at 800 rpm for 20 min at 25 °C. Collagen peptides were then dissolved in Milli-Q water at concentrations established in the factorial design, and TPP was prepared at 1.5 mg/mL, also in Milli-Q water.

The synthesis setup consisted of a peristaltic pump (Ecoshell® RD100-01, Pharr, TX, USA) delivering 5 mL of TPP at 5 mL/min dropwise into a vial containing 10 mL of chitosan solution, NaCl, Tween® 80, and curcumin (0.05 mg/mL), and 5 mL of collagen peptides (previously homogenized 15 min at 1100 rpm); after TPP addition, suspensions were stirred at 1100 rpm for 15 min [13]. The final systems were stored in glass vials (20 mL) at 4 °C without further drying or lyophilization. A 2^3 factorial design was applied to evaluate the influence of collagen peptides, NaCl, and Tween® 80 concentrations on nanoparticle properties (Table 1). The concentration ranges selected in this study were guided by previous reports from several authors [15–17], and the final pH ranged from 3.5 to 4.0.

Table 1. Experimental design for collagen-derived peptides, sodium chloride, and Tween 80® in nanoparticle synthesis.

Treatment	Components		
	Collagen-Derived Peptides (mg/mL)	**Sodium Chloride (M)**	**Tween 80® (µL)**
CL-SL-TL	2	0.15	100
CH-SL-TL	4	0.15	100
CL-SH-TL	2	0.30	100
CH-SH-TL	4	0.30	100
CL-SL-TH	2	0.15	200
CH-SL-TH	4	0.15	200
CL-SH-TH	2	0.30	200
CH-SH-TH	4	0.30	200

2.3. Particle Size Distribution

Mean particle size, polydispersity index (PDI), and size distribution were determined by dynamic light scattering (Zetasizer Nano ZS90, Malvern Instruments, Malvern, UK) at

25 °C and a fixed angle of 90°. For analysis, 1 mL of nanoparticle suspension was placed in a 1 cm glass cuvette. Measurements were performed in triplicate immediately after synthesis and weekly over 28 days of storage.

2.4. Zeta Potential

Zeta potential was measured using laser Doppler microelectrophoresis (Zetasizer Nano ZS90, Malvern Instruments, UK). For sample preparation, 1 mL of nanoparticle suspension was centrifuged at 12,000 rpm for 30 min (Eppendorf 5415C, Eppendorf, Germany); the pellet was then washed and resuspended in deionized water. From this suspension, 250 µL of washed nanoparticle suspension was mixed with 750 µL of deionized water and analyzed in a dip cell. Measurements were performed in triplicate immediately after synthesis and after 28 days for the most stable systems.

2.5. Encapsulation Efficiency

Encapsulation efficiency (EE) was determined indirectly by quantifying non-encapsulated curcumin in the supernatant [18]. One milliliter of nanoparticle suspension was centrifuged, and the supernatant was diluted up to 10 mL with ethanol (96%). The curcumin concentration was measured using UV-Vis spectrophotometry (λ = 425 nm, Agilent 8453, Santa Clara, CA, USA) using a calibration curve. EE (%) was calculated by comparing the initial curcumin content with the amount detected in the supernatant, using Equation (1):

$$\mathrm{EE}(\%) = \frac{\text{Initial amount}(\mathrm{mg}) - \text{Amount in supernatant}(\mathrm{mg})}{\text{Initial amount}(\mathrm{mg})} * 100, \quad (1)$$

Measurements were performed in triplicate for the most stable systems and a temperature of 25 °C was set for all evaluations.

2.6. In Vitro Antioxidant Activity

Both ABTS radical scavenging and ferric reducing antioxidant power (FRAP) activities were evaluated. ABTS radical scavenging activity was evaluated as described by Bhoopathy et al. [19]. The free radical solution was prepared by mixing ABTS (7 mM) and potassium persulfate (2.45 mM, 0.5:1 ratio), incubating this mixture for 16 h in the dark, and diluting it with ethanol to an absorbance of 0.800 ± 0.02 at 734 nm. Samples (250 µL of washed nanoparticle suspension) were mixed with 750 µL of $ABTS^{\bullet+}$ and then incubated for 6 min in the dark, and absorbance was measured at the same wavelength. A blank (deionized water) was used, and the percentage of radical inhibition was calculated using Equation (2):

$$\text{ABTS inhibition}(\%) = \left(\frac{\text{Absorbance}_{\text{Blank}} - \text{Absorbance}_{\text{Sample}}}{\text{Absorbance}_{\text{Blank}}}\right) * 100. \quad (2)$$

For the FRAP assay, solutions of TPTZ (10 mM in 40 mM HCl), $FeCl_3$ (20 mM in distilled water), and 0.3 mM acetate buffer (pH 3.6, adjusted with HCl) were prepared and maintained at 37 °C, then mixed in a 1:1:10 ratio (TPTZ/$FeCl_3$/buffer) to generate the radical solution [19]. Sample volumes were the same as in the ABTS assay and incubated in the dark at 37 °C for 30 min. Absorbance was measured at 593 nm, and the data were applied to Equation (3) to calculate the percentage of radical inhibition:

$$\text{FRAP inhibition}(\%) = \left(\frac{\text{Absorbance}_{\text{Sample}} - \text{Absorbance}_{\text{Blank}}}{\text{Absorbance}_{\text{Sample}}}\right) * 100. \quad (3)$$

2.7. In Vitro Anti-Inflammatory Activity

Anti-inflammatory activity was assessed through the inhibition of hemolysis under osmotic stress, following the method of Asif et al. [20]. Fresh blood was collected from healthy volunteers (no NSAID intake for ≥1 month) using EDTA Vacutainer® tubes. Erythrocytes were isolated by centrifugation at 1000 rpm for 5 min (Cole-Parmer 17250-10, Cole-Parmer®, Vernon Hills, IL, USA), plasma was removed, and the pellet was washed three times with saline solution. The final erythrocyte suspension (10% v/v) was prepared in PBS (pH 7.4; NaCl 138 mM, KCl 3 mM, Na_2HPO_4 8.1 mM, KH_2PO_4 1.5 mM).

Reaction mixtures (1 mL) contained 333 µL PBS, 667 µL hyposaline (NaCl 0.45%), 333 µL nanoparticle washed suspension, and 167 µL of erythrocytes (10% v/v). After incubation (30 min, 37 °C), samples were centrifuged (1000 rpm, 5 min) and supernatant absorbance was measured at 560 nm; PBS was used as the blank. Anti-inflammatory activity was calculated using Equation (4):

$$\text{Anti} - \text{inflammatory activity}(\%) = \left(\frac{\text{Absorbance}_{\text{Sample}} - \text{Absorbance}_{\text{Blank}}}{\text{Absorbance}_{\text{Sample}}} \right) * 100. \quad (4)$$

2.8. Statistical Analysis

Statistical analyses were carried out by analysis of variance (ANOVA) with Tukey's post hoc test (GraphPad Prism® 10). Significance was set at $p \leq 0.05$. Experiments were performed in triplicate and the results were expressed as mean ± standard deviation (SD).

3. Results and Discussion

3.1. Particle Size Distribution

Eight nanostructured systems were successfully prepared, showing a yellow color and slight opalescence, indicative of particle formation at the nanoscale [21]. All systems initially exhibited average particle sizes below 500 nm. As storage time progressed until reaching 28 days, two distinct behaviors were observed (Figure 1). The CH-SL-TL, CH-SL-TH, CL-SL-TL, and CL-SL-TH systems maintained a nearly constant particle size with no statistically significant differences ($p < 0.05$), indicating good colloidal stability. In contrast, the CH-SH-TL, CH-SH-TH, CL-SH-TL, and CL-SH-TH systems showed a progressive increase in particle size, reaching 1000–2000 nm by day 28.

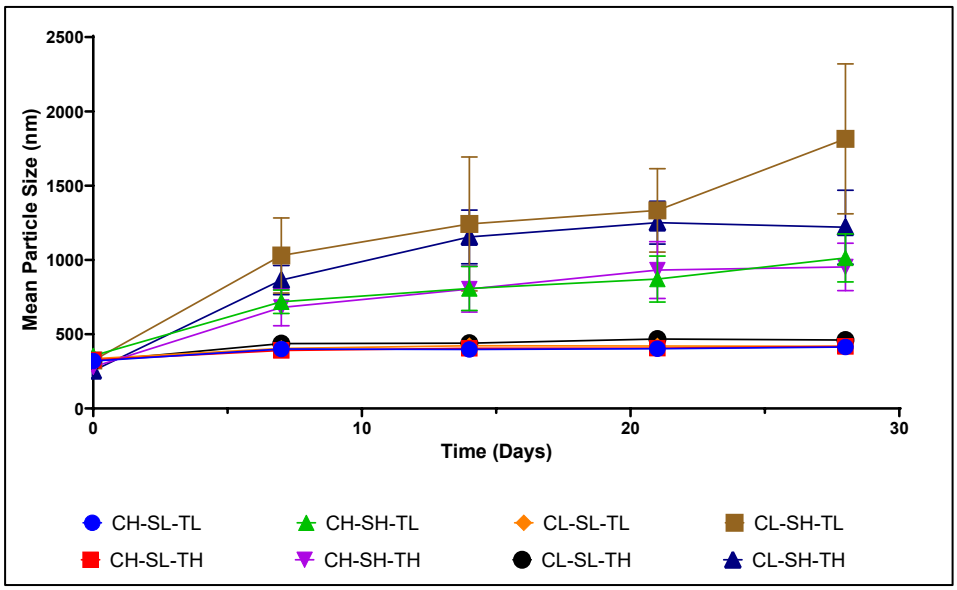

Figure 1. Mean particle size of chitosan nanoparticles during storage. Mean ± SD.

The observed instability in the high-NaCl systems (30 mM) highlights the critical role of ionic strength in nanoparticle formation. As reported by Sawtarie, Cai, and Lapitsky [17], NaCl can influence synthesis through two main mechanisms: (i) by reducing electrostatic repulsion, facilitating particle collisions, and (ii) by competing with TPP anions for chitosan binding, slowing particle formation and promoting aggregation. Both mechanisms are strongly concentration-dependent, where intermediate concentrations (~15–30 mM) can help control particle size and polydispersity, while higher concentrations (>50 mM) favor aggregation. In the present study, although NaCl may have contributed to particle homogeneity during synthesis, over time, its effect was offset by other stabilizing components, such as collagen-derived peptides, which enhance structural rigidity, and surfactants like Tween 80®, which prevent aggregation. Consequently, lower NaCl concentrations were sufficient to maintain stability in the presence of these stabilizers, which may be attributed to the osmotic effect that contributes to system stabilization.

The stable systems maintained particle sizes between 319.2 ± 23.5 and 461.0 ± 30.2 nm, values considered ideal and comparable to previous reports. Agarwal et al. [13] obtained ~168 nm nanoparticles using chitosan (0.5 mg/mL) and TPP (0.5 mg/mL), Anandhakumar et al. [15] reported ~100 nm with 5% (*w*/*v*) collagen peptides, Nair et al. [18] observed 251 nm with chitosan (0.2% *w*/*v*) and TPP (0.1% *w*/*v*), and Asif et al. [20] reported 481.7 nm when including 20 mM NaCl and Tween® 80. Findings confirm that the particle sizes obtained in this study are consistent with the expected range reported for comparable chitosan-based nanoparticle systems.

Due to the instability of the high-NaCl systems, only the CH-SL-TL, CH-SL-TH, CL-SL-TL, and CL-SL-TH systems were considered for further characterization. Additional stability parameters, including polydispersity index (PDI) and zeta potential, are presented in Table 2. PDI values remained largely unchanged over the evaluation period, further confirming the colloidal stability of these selected systems.

Table 2. Polydispersity index (PDI) and zeta potential of storage stable systems initially and after 28 days of evaluation.

Treatment	PDI (Adim.)		Zeta Potential (mV)	
	Day 0	Day 28	Day 0	Day 28
CH-SL-TL	0.243 ± 0.026 [a]	0.193 ± 0.023 [b]	51.34 ± 2.72 [a]	30.23 ± 5.14 [b]
CH-SL-TH	0.271 ± 0.017 [a]	0.222 ± 0.027 [b]	45.24 ± 4.90 [a]	30.78 ± 2.87 [b]
CL-SL-TL	0.226 ± 0.030 [a]	0.197 ± 0.032 [a]	41.12 ± 6.24 [a]	31.90 ± 3.50 [b]
CL-SL-TH	0.257 ± 0.018 [a]	0.218 ± 0.019 [b]	41.82 ± 4.65 [a]	31.32 ± 1.73 [b]

Means ± SD ($p < 0.05$). Equal letters in a row mean that there is no statistically significant difference.

3.2. Zeta Potential

The stability of nanoparticles prepared by ionic gelation with chitosan (CS) and sodium tripolyphosphate (TPP) is primarily attributed to the presence of protonated amino groups in the chitosan structure. These groups may not fully interact with TPP, either due to the relative amount of each component used in the synthesis or the spatial arrangement of the polymer within the nanoparticle matrix [18,22]. Treatments that exhibited good storage stability were further evaluated at initial and final time points to determine their zeta potential. In both cases, values above +25 mV were obtained, which fall within the stability range (<−25 mV or >+25 mV) reported by Duse et al. [21] and Sawtarie et al. [17], where electrostatic repulsion between particles prevents agglomeration.

Although zeta potential values remained within the stability range, a decrease from ~+50 mV to ~+30 mV was observed during storage. This reduction may be attributed to the availability of amino groups from CS as well as interactions with collagen-derived peptides, where differences in zeta potential values can be associated with variations in component

concentrations, as their interactions directly influence nanoparticle synthesis and stability. Comparable values have been reported by Nair et al. [18], who obtained a zeta potential of +20.23 mV using for nanoparticle synthesis 0.2% (*w*/*v*) CS, 0.1% (*w*/*v*) TPP, and 0.5 mg/mL curcumin; nevertheless, no evaluation of zeta potential or size during storage was reported.

3.3. Encapsulation Efficiency

The encapsulation efficiency (EE) of curcumin in the evaluated systems ranged between ~38–60%, equivalent to concentrations of 18–29 µg/mL (CH-SL-TL, 57.6 ± 0.76%; CH-SL-TH, 58.23 ± 1.25%; CL-SL-TL, 44.09 ± 7.88%; and CL-SL-TH, 39.44 ± 2.10%). Although these values are lower than those typically reported for ionic gelation (75–80%), similar efficiencies (45–60%) have been observed in formulation with similarities in composition and the nature of different compounds [20]. Variations in EE may be attributed to the nature of the components, as phosphate and hydroxyl groups enhance interactions between the anionic groups of TPP and the protonated amino groups of chitosan, thereby improving curcumin retention within the nanoparticles [16,19,21]. However, at high concentrations, these interactions may lead to polymer sedimentation.

In most cases, changes in EE are associated with particle size increase, since CS and TPP can continue interacting in solution, promoting higher encapsulation as the system stabilizes [19]. Additionally, curcumin may not be confined solely within the nanoparticle core but also adsorbed onto its surface through interactions with protonated amino groups of chitosan, as suggested by Asif et al. [20] and Boruah et al. [16].

3.4. Antioxidant Activity

Two main mechanisms are involved in antioxidant assays: hydrogen atom transfer (HAT) and electron transfer (ET) [23]. Given that curcumin displays both mechanisms, ABTS and FRAP assays were performed to evaluate its activity. Nanoparticles showed ABTS inhibition values between 20% and 35%, with effective encapsulated curcumin concentrations ranging from 18 to 29 µg/mL (Figure 2a). These results are higher than those reported by Mošovská et al. [24], who found an inhibition of 15–16% with phospholipid systems, 14–18% with cyclodextrins, and 11–14% for free curcumin, suggesting that collagen peptide derivatives may enhance encapsulation efficiency and bioactivity [25,26]. Similarly, Bhoopathy et al. [19] reported ~35.34% inhibition using chitosan/TPP nanoparticles (EE = 77.53%), while Alhajamee et al. [27] observed ~30% inhibition with a chitosan–lipid–ethanol system containing 184 µg/mL of curcumin. Comparisons suggest that variations in nanoparticle composition and component concentration influence response and antioxidant performance.

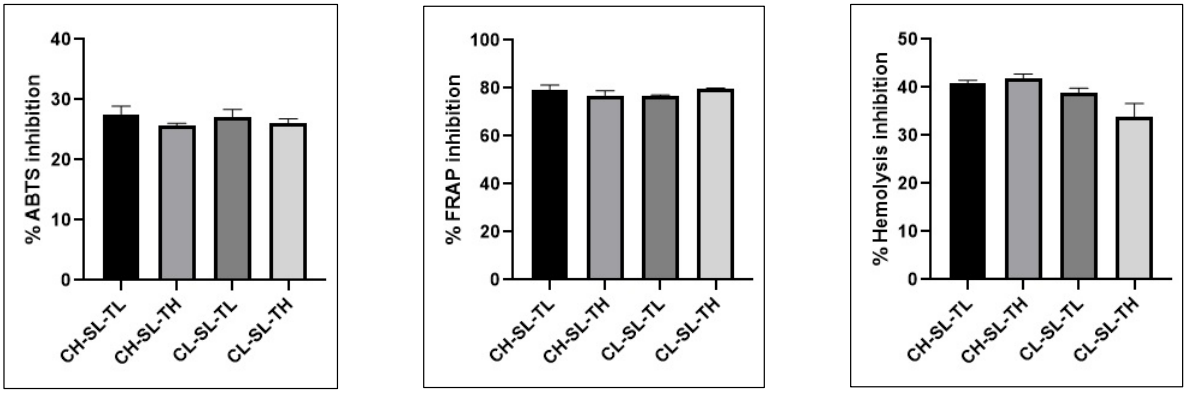

(**a**) (**b**) (**c**)

Figure 2. (**a**) ABTS antioxidant assay. (**b**) FRAP antioxidant assay. (**c**) Hypotonic-induced hemolysis assay of stable systems. Means ± SD ($p < 0.05$).

In the FRAP assay, inhibition ranged from 60% to 80% (Figure 2b), exceeding the 44–54% reported by Mošovská et al. [24] for curcumin encapsulated in cyclodextrins, 43–47% in phospholipid systems, and 39–48% for free curcumin at equivalent concentrations. Improvement in activity may be attributed to the presence of chitosan, collagen-derived peptides, surfactants, and salts, which can contribute to the overall antioxidant effect, suggesting that not only curcumin but also the encapsulating vehicle enhances bioactivity [25,26,28].

3.5. Anti-Inflammatory Activity

An indirect method for evaluating anti-inflammatory activity is in vitro hemolysis inhibition under hypotonic conditions. In this study, the evaluated treatments showed inhibition values ranging from 30% to 40% (Figure 2c). These results are comparable to those reported by Asif et al. [20], who, using a Tween® 80–TPP–chitosan formulation with 200 μg/mL of curcumin-loaded nanoparticles and 200 μg/mL of free curcumin, observed inhibition rates of 30% and 28%, respectively. In another study, Singh et al. [29] demonstrated 50–70% inhibition when 20 μg/mL of curcumin dissolved in DMSO was tested against *Vibrio cholerae* protein-induced hemolysis. Considering these comparisons, the curcumin nanoparticles developed in the present work exhibit significant anti-inflammatory potential compared to drugs such as diclofenac. This is probably due to their ability to protect cell membranes and reduce oxidative damage under stress conditions. Since the systems are complex mixtures of multiple compounds, the observed bioactivity cannot be attributed solely to curcumin, but the increased activity could be due to nanoencapsulation. Nanostructured systems have been shown to exceed the activity of free curcumin, achieving similar or greater inhibition at lower concentrations of bioactive compounds [20].

4. Conclusions

Our results highlight the importance of using NaCl in nanoparticle formulation and its effect on storage stability, as it regulates particle synthesis. We identified optimal formulations in which the combination of Tween® 80, collagen peptide derivatives, and salt generates stable nanoparticles with sizes suitable for administration and appropriate encapsulation efficiencies, making them carrier systems for bioactive compounds such as curcumin. Future work should address their release kinetics, bioavailability, and biological performance to further assess their applicability in nutraceutical, cosmetic, and pharmaceutical formulations.

Author Contributions: Conceptualization, M.I.-A., C.U.R.-F. and C.C.-S.; methodology, C.U.R.-F.; validation, C.U.R.-F., A.V.-P. and C.C.-S.; formal analysis, M.I.-A. and C.U.R.-F.; investigation, M.I.-A.; resources, C.C.-S.; data curation, C.U.R.-F. and A.V.-P.; writing—original draft preparation, M.I.-A. and C.U.R.-F.; writing—review and editing, A.V.-P. and C.C.-S.; supervision, C.C.-S.; project administration, C.C.-S.; funding acquisition, C.C.-S. All authors have read and agreed to the published version of the manuscript.

Funding: This research received no external funding.

Institutional Review Board Statement: This study was conducted in accordance with Mexican regulations for health research and approved by the research committee of the Tecnológico Nacional de México (CITEC) (CITEC/ITVER/No.07/2024 approved on 17 January 2024).

Informed Consent Statement: Informed consent was obtained from all subjects involved in the study.

Data Availability Statement: The data that support the findings of this study are available on request from the corresponding author.

Conflicts of Interest: The authors declare no conflicts of interest.

References

1. Jayaprakasha, G.K.; Jagan Mohan Rao, L.; Sakariah, K.K. Chemistry and biological activities of *C. longa*. *Trends Food Sci. Technol.* **2005**, *16*, 533–548. [CrossRef]
2. Amalraj, A.; Pius, A.; Gopi, S.; Gopi, S. Biological activities of curcuminoids, other biomolecules from turmeric and their derivatives—A review. *J. Tradit. Complement. Med.* **2017**, *7*, 205–233. [CrossRef]
3. Hewlings, S.J.; Kalman, D.S. Curcumin: A Review of Its Effects on Human Health. *Foods* **2017**, *6*, 92. [CrossRef]
4. Thiagarajan, R.; Manikandan, R. Antioxidants and cataract. *Free Radic. Res.* **2013**, *47*, 337–345. [CrossRef]
5. Patel, S.R.; Lin, A.S.P.; Edelhauser, H.F.; Prausnitz, M.R. Suprachoroidal Drug Delivery to the Back of the Eye Using Hollow Microneedles. *Pharm. Res.* **2011**, *28*, 166–176. [CrossRef]
6. Weiss, J.; Takhistov, P.; McClements, D.J. Functional Materials in Food Nanotechnology. *J. Food Sci.* **2006**, *71*, R107–R116. [CrossRef]
7. Sajid, M.; Płotka-Wasylka, J. Nanoparticles: Synthesis, characteristics, and applications in analytical and other sciences. *Microchem. J.* **2020**, *154*, 104623. [CrossRef]
8. Khan, Y.; Sadia, H.; Ali Shah, S.Z.; Khan, M.N.; Shah, A.A.; Ullah, N.; Ullah, M.F.; Bibi, H.; Bafakeeh, O.T.; Khedher, N.B.; et al. Classification, Synthetic, and Characterization Approaches to Nanoparticles, and Their Applications in Various Fields of Nanotechnology: A Review. *Catalysts* **2022**, *12*, 1386. [CrossRef]
9. Zielińska, A.; Carreiró, F.; Oliveira, A.M.; Neves, A.; Pires, B.; Venkatesh, D.N.; Durazzo, A.; Lucarini, M.; Eder, P.; Silva, A.M.; et al. Polymeric Nanoparticles: Production, Characterization, Toxicology and Ecotoxicology. *Molecules* **2020**, *25*, 3731. [CrossRef] [PubMed]
10. Pedroso-Santana, S.; Fleitas-Salazar, N. Ionotropic gelation method in the synthesis of nanoparticles/microparticles for biomedical purposes. *Polym. Int.* **2020**, *69*, 443–447. [CrossRef]
11. Silvestro, I.; Francolini, I.; Di Lisio, V.; Martinelli, A.; Pietrelli, L.; Scotto d'Abusco, A.; Scoppio, A.; Piozzi, A. Preparation and Characterization of TPP-Chitosan Crosslinked Scaffolds for Tissue Engineering. *Materials* **2020**, *13*, 3577. [CrossRef] [PubMed]
12. Yetisgin, A.A.; Cetinel, S.; Zuvin, M.; Kosar, A.; Kutlu, O. Therapeutic Nanoparticles and Their Targeted Delivery Applications. *Molecules* **2020**, *25*, 2193. [CrossRef]
13. Agarwal, M.; Shrivastav, N.; Pandey, S.; Das, R.; Gaur, P. Preparation of Chitosan Nanoparticles and their In-vitro Characterization. *Int. J. Life-Sci. Sci. Res.* **2018**, *4*, 1713–1720. [CrossRef]
14. Ozturk, K.; Arslan, F.B.; Tavukcuoglu, E.; Esendagli, G.; Calis, S. Aggregation of chitosan nanoparticles in cell culture: Reasons and resolutions. *Int. J. Pharm.* **2020**, *578*, 119119. [CrossRef]
15. Anandhakumar, S.; Krishnamoorthy, G.; Ramkumar, K.M.; Raichur, A.M. Preparation of collagen peptide functionalized chitosan nanoparticles by ionic gelation method: An effective carrier system for encapsulation and release of doxorubicin for cancer drug delivery. *Mater. Sci. Eng. C* **2017**, *70*, 378–385. [CrossRef]
16. Boruah, B.; Saikia, P.M.; Dutta, R.K. Binding and stabilization of curcumin by mixed chitosan–surfactant systems: A spectroscopic study. *J. Photochem. Photobiol. A Chem.* **2012**, *245*, 18–27. [CrossRef]
17. Sawtarie, N.; Cai, Y.; Lapitsky, Y. Preparation of chitosan/tripolyphosphate nanoparticles with highly tunable size and low polydispersity. *Colloids Surf. B Biointerfaces* **2017**, *157*, 110–117. [CrossRef]
18. Nair, R.S.; Morris, A.; Billa, N.; Leong, C.-O. An Evaluation of Curcumin-Encapsulated Chitosan Nanoparticles for Transdermal Delivery. *AAPS PharmSciTech* **2019**, *20*, 69. [CrossRef]
19. Bhoopathy, S.; Inbakandan, D.; Rajendran, T.; Chandrasekaran, K.; Kasilingam, R.; Gopal, D. Curcumin loaded chitosan nanoparticles fortify shrimp feed pellets with enhanced antioxidant activity. *Mater. Sci. Eng. C* **2021**, *120*, 111737. [CrossRef] [PubMed]
20. Asif, H.M.; Zafar, F.; Ahmad, K.; Iqbal, A.; Shaheen, G.; Ansari, K.A.; Rana, S.; Zahid, R.; Ghaffar, S. Synthesis, characterization and evaluation of anti-arthritic and anti-inflammatory potential of curcumin loaded chitosan nanoparticles. *Sci. Rep.* **2023**, *13*, 10274. [CrossRef] [PubMed]
21. Duse, L.; Baghdan, E.; Pinnapireddy, S.R.; Engelhardt, K.H.; Jedelská, J.; Schaefer, J.; Quendt, P.; Bakowsky, U. Preparation and Characterization of Curcumin Loaded Chitosan Nanoparticles for Photodynamic Therapy. *Phys. Status Solidi (A)* **2018**, *215*, 1700709. [CrossRef]
22. Valencia, M.S.; Silva Júnior, M.F.d.; Xavier-Júnior, F.H.; Veras, B.d.O.; Albuquerque, P.B.S.d.; Borba, E.F.d.O.; Silva, T.G.d.; Xavier, V.L.; Souza, M.P.d.; Carneiro-da-Cunha, M.d.G. Characterization of curcumin-loaded lecithin-chitosan bioactive nanoparticles. *Carbohydr. Polym. Technol. Appl.* **2021**, *2*, 100119. [CrossRef]
23. Vora, D.; Heruye, S.; Kumari, D.; Opere, C.; Chauhan, H. Preparation, Characterization and Antioxidant Evaluation of Poorly Soluble Polyphenol-Loaded Nanoparticles for Cataract Treatment. *AAPS PharmSciTech* **2019**, *20*, 163. [CrossRef]
24. Mošovská, S.; Petáková, P.; Kaliňák, M.; Mikulajová, A. Antioxidant properties of curcuminoids isolated from *Curcuma longa* L. *Acta Chim. Slovaca* **2016**, *9*, 130–135. [CrossRef]
25. Arun, A.; Malrautu, P.; Laha, A.; Luo, H.; Ramakrishna, S. Collagen Nanoparticles in Drug Delivery Systems and Tissue Engineering. *Appl. Sci.* **2021**, *11*, 11369. [CrossRef]

26. Guo, H.; Hong, Z.; Yi, R. Core-Shell Collagen Peptide Chelated Calcium/Calcium Alginate Nanoparticles from Fish Scales for Calcium Supplementation. *J. Food Sci.* **2015**, *80*, N1595–N1601. [CrossRef] [PubMed]
27. Alhajamee, M.; Marai, K.; Al Abbas, S.M.N.; Homayouni Tabrizi, M. Co-encapsulation of curcumin and tamoxifen in lipid-chitosan hybrid nanoparticles for cancer therapy. *Mater. Technol.* **2022**, *37*, 1183–1194. [CrossRef]
28. Zhang, X.; Li, Y.; Guo, M.; Jin, T.Z.; Arabi, S.A.; He, Q.; Ismail, B.B.; Hu, Y.; Liu, D. Antimicrobial and UV Blocking Properties of Composite Chitosan Films with Curcumin Grafted Cellulose Nanofiber. *Food Hydrocoll.* **2021**, *112*, 106337. [CrossRef]
29. Singh, M.; Rupesh, N.; Pandit, S.B.; Chattopadhyay, K. Curcumin Inhibits Membrane-Damaging Pore-Forming Function of the β-Barrel Pore-Forming Toxin Vibrio cholerae Cytolysin. *Front. Microbiol.* **2022**, *12*, 809782. [CrossRef]

Disclaimer/Publisher's Note: The statements, opinions and data contained in all publications are solely those of the individual author(s) and contributor(s) and not of MDPI and/or the editor(s). MDPI and/or the editor(s) disclaim responsibility for any injury to people or property resulting from any ideas, methods, instructions or products referred to in the content.